Bull Eng Geol Environ (2017) 76:1107–1115
DOI 10.1007/s10064-016-0893-3

ORIGINAL PAPER

Estimating the uniaxial compressive strength of pyroclastic rocks from the slake durability index

Sair Kahraman[1] · Mustafa Fener[2] · Osman Gunaydin[3]

Received: 22 January 2016 / Accepted: 22 April 2016 / Published online: 3 May 2016

Abstract Because the preparation of standard samples may not always be possible for weak or soft rocks, the prediction of uniaxial compressive strength (UCS) from indirect methods is widely used for preliminary investigations. In this study, the possibility of predicting UCS from the slake durability index (SDI) was investigated for pyroclastic rocks. For this purpose, pyroclastic rocks were collected from 31 different locations in the Cappadocian Volcanic Province of Turkey. The UCS and SDI tests were carried out on the samples in the laboratory. The UCS values were correlated with the SDI values and a very strong exponential relation was found between the two parameters. Since some data were scattered over the UCS values of 20 MPa, the correlation plot was redrawn for above and below the UCS values of 20 MPa, respectively. Very strong linear correlations were developed for two cases. Our concluding remark is that the UCS of pyroclastic rocks can be estimated from the SDI.

Keywords Uniaxial compressive strength · Slake durability index · Pyroclastic rocks · Empirical equations

✉ Sair Kahraman
sairkahraman@yahoo.com

1 Mining Engineering Department, Hacettepe University, Ankara, Turkey

2 Geological Engineering Department, Ankara University, Ankara, Turkey

3 Civil Engineering Department, Adiyaman University, Adiyaman, Turkey

Introduction

Rock engineers widely use the uniaxial compressive strength (UCS) of rock in designing surface and underground structures. Although the procedure of measuring this rock strength is relatively simple, it is time consuming and expensive. Also, it requires well-prepared rock cores. Therefore, indirect tests are often used to predict UCS, such as the Schmidt rebound number, point load index, impact strength, and sound velocity, especially for preliminary studies. However, preparing standard samples for some indirect test may not always be possible for weak or soft rocks. The slake durability test is a cheap and easy test to carry out and requires very little sample preparation. It may be an indirect measure of the UCS of rock if significant correlations are derived.

The literature review shows that the studies on the relation between UCS and SDI are very limited and there is no research on pyroclastic rocks. In this study, the relation between UCS and SDI was investigated for pyroclastic rocks collected from 31 different locations.

Previous studies

Some researchers have investigated the relation between UCS and slake durability index (SDI) to develop an estimation equation for UCS. Bonelli (1989) investigated the correlation between the UCS and SDI for sandstones but did not find any correlation. This is probably due to the fact that the SDI test is useful for weak rocks.

Cargill and Shakoor (1990) performed the UCS and SDI tests on different rocks (sandstone, limestone, marble dolomite, and syenite) and correlated the two rock properties. They derived the following equation:

$$UCS = 60.34 I_{d2} - 5822 \quad r = 0.74 \tag{1}$$

where UCS is uniaxial compressive strength (MPa), and I_{d2} is the two-cycle SDI (%).

Koncagul and Santi (1999) investigated the predictability of UCS from SDI for the Breathitt shale. They correlated UCS with SDI and found the following equation:

$$UCS = 0.658 I_{d2} + 9.081 \quad r = 0.63 \tag{2}$$

where UCS is uniaxial compressive strength (MPa), and I_{d2} is the two-cycle SDI (%).

The data points are fairly scattered in the correlation graph plotted by Koncagul and Santi (1999) and the correlation coefficient is not strong. They also stated that the SDI values above 94 % show a wide range of UCS for a narrow range of durability.

Gokceoglu et al. (2000) investigated the influence of mineralogy and strength on the durability of different types of weak and clay-bearing rocks selected from Turkey. They also correlated UCS to SDI and did not find a meaningful correlation between the two parameters for all tested rock types. They repeated the correlation analysis for only marls and derived the following equation:

$$UCS = 2.54 I_{d4} - 202 \quad r = 0.76 \tag{3}$$

where UCS is uniaxial compressive strength (MPa), and I_{d4} is the four-cycle SDI (%).

Dincer et al. (2008) aimed at developing some prediction equations for UCS and Young's modulus from index tests and physical properties for Quaternary caliche deposits. They derived the following relations between UCS and SDI:

$$UCS = 0.211 I_{d2} - 13.815 \quad r = 0.68 \tag{4}$$

$$UCS = 13.636 \ln I_{d2} - 69.552 \quad r = 0.65 \tag{5}$$

$$UCS = 4.9 \times 10^{-7} I_{d2}^{3.578} \quad r = 0.74 \tag{6}$$

$$UCS = 0.084 e^{0.45 I_{d2}} \quad r = 0.76 \tag{7}$$

where UCS is uniaxial compressive strength (MPa), and I_{d2} is the two-cycle SDI (%).

Yagiz (2011) studied the correlations between SDI and some rock properties for carbonate rocks. He found a strong linear correlation between UCS and SDI. The equation of the correlation is as follows:

$$UCS = 29.63 I_{d4} - 2858 \quad r = 0.94 \tag{8}$$

where UCS is uniaxial compressive strength (MPa), and I_{d4} is the four-cycle SDI (%).

Geology and mineralogy

The block samples of pyroclastic rocks were collected from the 31 different locations in the Cappadocian Volcanic Province (CVP) (Table 1). The CVP is located in central Anatolia (Fig. 1). It extends as a belt in the NE-SW direction with a long axis of about 300 km and is in large part situated within the Anatolide tectonic belt. The main units in the province are basement rocks, Yeşilhisar Formation, Ürgüp Formation, and Quaternary deposits. The Ürgüp Formation corresponds to Mio-Pliocene ignimbritic volcaniclastic rocks intercalated with sediments of lacustrine and fluvial facies. It has a thickness of more than 400 m and extends throughout the CVP. It consists of seven ignimbritic members (Kavak, Zelve, SarımadenTepe, Cemilköy, Tahar, Gördeles and Kızılkaya), and two lava flows (Damsa and Topuzdag) intercalated with sedimentary rocks (Çökek Member). The ignimbritic members related to this study are explained in the following (Sayin 2008):

The Kavak Ignimbrite is generally non-welded and sometimes includes ash fall and ash cloud layers. A very evident feature of the Kavak Ignimbrite is its characteristic erosional forms of fairy chimneys and sweeping curves extending through an area of over 100 km^2 with the principal centers at Ürgüp, Üçhisar, Ortahisar, and Göreme.

The Zelve Ignimbrite consists of non-welded ignimbrite. This unit is characterized by pink color ignimbrite and an extensive basal white colored air fall (pumice fall) deposit. This fallout layer, 4–15 m thick, is a good stratigraphic marker horizon, which defines the boundary between the Kavak and Zelve Ignimbrites. This horizon contributes to the formation of well-known "capped" fairy chimneys around Zelve village.

Sarımaden Tepe Ignimbrite consists of welded pyroclastic flow deposit in several localities. An air fall deposit exists at the bottom of the unit. It characteristically displays a vertical variation from a white color at the basal part to a dark gray or dark brown at the middle part and to a light pinkish color at the upper part. The thickness of this member is 5–15 m in the study area. It is exposed in Sarımaden Tepe, Orta Tepe, Bucak Kepez Tepe, Üçhisar Dağ, in the northeast of Çardak Village, and Ören Tepe, Karanlık Tepe and Karakaya Tepe in the southeast of Çardak Village, south of Mustafapaşa and Ayvalı villages.

The Cemilköy Ignimbrite is observed in the Damsa valley (Cemilköy, Taşkınpaşa, and Şahinefendi villages) and south of Ayvalı village. It is about 100 m thick in Cemilköy village. It comprises a generally massive light cream or light gray single ash flow unit representing the main body and a fine grained basal part with fine-grained

Table 1 Mineralogical and structural properties of samples

Rock code	Sample location	Petrographic name	Mineralogical content	Structural properties
1	Derbent-1/ Nigde	Altered ignimbrite	2 % Quartz 1 % Pyroxene 23 % Rock fragments 74 % Matrix	Very coarse-grained orthoclase and microcline phenocrysts Typically, pink and red colored orthoclase is the predominant mineral, showing perthitic texture Subhedral to anhedral plagioclase, polysynthetic albite twinning and distinctively zoned subhedral to euhedral plagioclase crystals (albite), anhedral quartz
2	Dere Mah.-1/ Nigde	Lithic tuff	16 % Plagioclase 9 % Pyroxene 20 % Rock fragments 55 % Matrix	Hyaloporphiric texture Subhedral to euhedral plagioclases and rock fragments are dispersed in matrix Pyroxenes are rich in cracks and seen as small crystals in the matrix Matrix is generally made up of pumice and volcanic shards
3	Dere Mah.-2/ Nigde	Altered ignimbrite	Undefined	Severely altered under the effect of hydrothermal solutions Iron oxide and clay formations are seen also in matrix and rock fragments
4	Kiziloren/ Nigde	Ignimbrite	11 % Plagioclase 3 % Pyroxene 7 % Biotite 5 % Rock fragments 74 % Matrix	Hyaloporphyric to hypocrystalline textures Subhedral to euhedral plagioclases and rock fragments are dispersed in matrix Biotites are seen as platy shapes and generally altered Rock fragments are generally from plutonic rocks Matrix is generally made up of pumice and volcanic shards
5	Ozbelde/Nigde	Altered ignimbrite	Undefined	Severely altered under the effect of hydrothermal solutions Iron oxide and clay formations are seen also in matrix and rock fragments
6	Aktas-1/Nigde	Ignimbrite	15 % Plagioclase 4 % Biotite 1 % Pyroxene 38 % Rock fragments 42 % Matrix	Hyaloporphyric to hypocrystalline textures Sericite formation can be seen within biotites Subhedral to euhedral plagioclases and rock fragments are dispersed in matrix Matrix is generally made up of pumice and volcanic shards Chalcedony formations
7	Aktas-2/Nigde	Crystal Tuff	14 % Plagioclase 7 % Pyroxene 1 % Biotite 7 % Rock fragments 71 % Matrix	Hyaloporphyric to hypocrystalline textures Anhedral plagioclases and pyroxene minerals dispersed in matrix Matrix is generally made up of pumice Zircon minerals are seen as accessory minerals
8	Derinkuyu/ Nevsehir	Ignimbrite	7 % Quartz 2 % Biyotit 4 % Rock fragments 87 % Matrix	Hypocrystalline texture Anhedral quartz minerals in matrix More felsic in composition Carbonate formation can be seen in biotites Matrix is generally made up of pumice and volcanic shards
9	Karayazi/ Nevsehir	Ignimbrite	3 % Quartz 2 % Biyotit 20 % Rock fragments 75 % Matrix	Hyaloporphyrictexture Subhedral quartz minerals in matrix Sericite formation can be seen in biotites Chalcedony formation and zircon minerals Matrix is generally made up of pumice and volcanic shards
10	Bahceli/Nigde	Ignimbrite	8 % Plagioclase 2 % Biotite 4 % Quartz 2 % Pyroxene 4 % Rock fragments 80 % Matrix	Hyaloporphyric to hypocrystalline textures Subhedral plagioclase in matrix Pyroxene and biotite minerals are rich in cracks Anhedral quartz minerals Matrix is made up of pumice and volcanic shards

Table 1 continued

Rock code	Sample location	Petrographic name	Mineralogical content	Structural properties
11	Gumusler/ Nigde	Ignimbrite	7 % Quartz 15 % Plagioclase 4 % Biotite 15 % Rock fragments 59 % Matrix	Hyaloporphyric to hypocrystalline textures Subhedral to euhedral plagioclases and rock fragments are dispersed in matrix Biotites are seen as platy shapes and generally altered Anhedral quartz minerals, Matrix is generally made up of pumice and volcanic shards Minor zircon and talc minerals
12	Tomarza/ Kayseri	Ignimbrite	7 % Quartz 12 % Plagioclase 2 % Biotite 25 % Rock fragments 55 % Matrix	Hyaloporphyric texture Subhedral to euhedral plagioclases and rock fragments are dispersed in matrix Rocks fragments are generally from metamorphic rocks Intense carbonate formation Matrix is generally made up of pumice and volcanic shards
13	Tomarza/ Kayseri	Ignimbrite	7 % Plagioclase 3 % Pyroxene 6 % Rock fragments 74 % Matrix	Hyaloporphyric texture Subhedral to euhedral plagioclases and rock fragments are dispersed in matrix Pyroxene are rich in cracks Iron oxide formation in the matrix Matrix is generally made up of pumice and volcanic shards
14	Avanos/ Nevsehir	Ignimbrite	8 % Quartz 3 % Pyroxene 13 % Rock fragments 76 % Matrix	Hyaloporphyric to hypocrystalline textures Anhedral quartz minerals dispersed in matrix Carbonate formation can be seen in mafic minerals Matrix is made up of pumice and volcanic shards
15	Derbent-2/ Nigde	Altered ignimbrite	Undefined	Severely altered under the effect of hydrothermal solutions Iron oxide and clay formations are seen also in matrix and rock fragments
16	Gulluce/Nigde	Altered ignimbrite	Undefined	Severely altered under the effect of hydrothermal solutions Iron oxide and clay formations are seen also in matrix and rock fragments
17	Arapli/Nigde	Ignimbrite	5 % Quartz 16 % Plagioclase 6 % Biotite 3 % Rock fragments 70 % Matrix	Hyaloporphyric to hypocrystalline textures Subhedral to euhedral plagioclases and rock fragments are dispersed in matrix Anhedral quartz minerals Carbonate formation is seen in matrix Matrix is made up of pumice and volcanic shards
18	Mustafapasa/ Nevsehir	Ignimbrite	8 % Plagioclase 3 % Quartz 2 % Pyroxene 13 % Rock fragments 66 % Matrix	Hyaloporphyric to hypocrystalline textures Subhedral plagioclase minerals dispersed in matrix Anhedral quartz minerals in matrix Matrix is generally made up of pumice and volcanic shards
19	Incesu/Kayseri	Ignimbrite	7 % Plagioclase 2 % Pyroxene 9 % Rock fragments 82 % Matrix	Hyaloporphyric to hypocrystalline textures Subhedral to euhedral plagioclases and rock fragments are dispersed in matrix Minor zircon minerals in matrix Matrix is generally made up of pumice and volcanic shards
20	Avanos/ Nevsehir	Pumice	5 % Quartz 6 % Plagioclase 89 % Matrix	Hyaloporphyric texture Chalcedony formations Anhedral plagioclases in matrix Composition is generally pumice

Table 1 continued

Rock code	Sample location	Petrographic name	Mineralogical content	Structural properties
21	Karayazi/ Nevsehir	Ignimbrite	6 % Quartz 3 % Biotite 22 % Rock fragments 69 % Matrix	Hyaloporphyric to hypocrystalline textures Sericite formation in biotites Anhedral quartz minerals in matrix Iron oxide and clay formation in matrix Matrix is generally made up of pumice and volcanic shards
22	Karayazi/ Nevsehir	Ignimbrite	2 % Quartz 3 % Biotite 33 % Rock fragments 62 % Matrix	Hyaloporphyric to hypocrystalline textures Subhedral to euhedral plagioclases and rock fragments are dispersed in matrix Carbonate formation in biotites Matrix is generally made up of pumice and volcanic shards
23	Karayazi/ Nevsehir	Ignimbrite	6 % Quartz 2 % Biotite 5 % Rock fragments 87 % Matrix	Hyaloporphyrictexture Euhedral and anhedral quartz minerals in matrix Carbonate formation in biotites More felsic in chemical composition Matrix is made up of pumice and volcanic shards
24	Karayazi/ Nevsehir	Tuff	7 % Quartz 20 % Chalcedony 11 % Rock fragments 62 % Matrix	Hypocrystalline texture Severe clay formation in matrix Chalcedony formation
25	Karayazi/ Nevsehir	Ignimbrite	2 % Quartz 2 % Pyroxene 17 % Rock fragments 70 % Matrix	Hyaloporphyric texture Iron oxide formation in matrix Matrix is made up of pumice and volcanic shards
26	Tomarza/ Kayseri	Ignimbrite	6 % Plagioclase 3 % Pyroxene 22 % Rock fragments 69 % Matrix	Hyaloporphyric to hypocrystalline textures Anhedral quartz minerals dispersed in matrix Subhedral to euhedral plagioclases and rock fragments are dispersed in matrix Chalcedony formation Matrix is made up of pumice and volcanic shards
27	Selime/ Aksaray	Ignimbrite	3 % Quartz 7 % Plagioclase 3 % Biotite 11 % Rock fragments 76 % Matrix	Hyaloporphyric to hypocrystalline textures Anhedral quartz minerals dispersed in matrix Subhedral to euhedral plagioclases and rock fragments are dispersed in matrix Sericite formation in biotites Chalcedony formation Matrix is made up of pumice and volcanic shards
28	Taspinar/ Aksaray	Tuff	4 % Quartz 12 % Plagioclase 3 % Biotite 8 % Rock fragments 73 % Matrix	Hyaloporphyric texture Anhedral quartz minerals dispersed in matrix Sericite formation in biotites Carbonate formation is common in matrix Carbonated unmerged tuff
29	Altunhisar/ Nigde	Crystal Tuff	8 % Quartz 35 % Plagioclase 4 % Biotite 5 % Rock fragments 48 % Matrix	Hypocrystalline textures Subhedral to euhedral plagioclases and rock fragments are dispersed in matrix Crystallite + microlites in matrix

Table 1 continued

Rock code	Sample location	Petrographic name	Mineralogical content	Structural properties
30	Persek/Kayseri	Ignimbrite	3 % Pyroxene	Hyaloporphyric texture
			10 % Plagioclase	Subhedral to euhedral plagioclases and rock fragments are dispersed in matrix
			35 % Rock fragments	Pyroxene are rich in cracks
			52 % Matrix	Iron oxide formation in the matrix
				Matrix is generally made up of pumice and volcanic shards
31	Basakpinar/ Kayseri	Ignimbrite	4 % Pyroxene	Hyaloporphyric texture
			19 % Plagioclase	Subhedral to euhedral plagioclases and rock fragments are dispersed in matrix
			24 % Rock fragments	Pyroxene are rich in cracks
			76 % Matrix	Iron oxide formation in the matrix
				Matrix is generally made up of pumice and volcanic shards

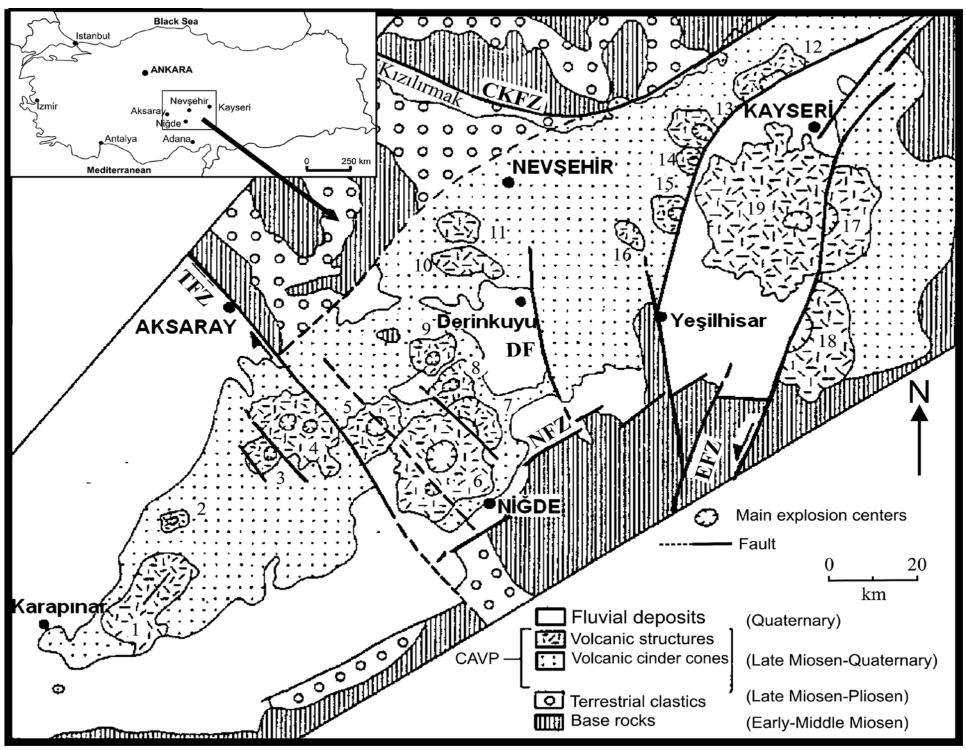

Fig. 1 Simplified geological map of the Cappadocian Volcanic Province (CVP). Numbers show the major volcanic complexes: *1*. Karacadag volcanics, *2*. Kotudag volcanics, *3*. Kecikalesi volcanics, *4*. Hasandag volcanics, *5*. Keciboyduran volcanics, *6*. Melendiz volcanics, *7*. Tepekoy volcanics, *8*. Cinarli volcanics, *9*. Golludag volcanics, *10*. Acigol volcanics, *11*. Kizilcin volcanics, *12*. Erkilet volcanics, *13*. Hamurcu volcanics, *14*. Seksenveren volcanics, *15*. Tekkedag volcanics, *16*. Hoduldag volcanics, *17*. Kocdag volcanics, *18*. Develidag volcanics, *19*. Erciyes volcanics (Toprak et al. 1994)

pumice particles and ash cloud (surge) deposits at the bottom.

The Tahar Ignimbrite consists of pinkish to cream non-welded ignimbrite and is underlain and overlain by continental sediments of the Çökek Member. It is observed on both sides of the Damsa valley in the study area. The thickness of the Ignimbrite is 5–15 m in the area, but locally reaches 80 m.

The Gördeles Ignimbrite is located stratigraphically between the Kızılkaya and Tahar Ignimbrites and is exposed on both sides of the Damsa valley and in the southern parts of Ayvalı villages. It comprises mainly light gray to pinkish ash flow units (ignimbrite), which are non-welded and partly welded ignimbrite. It is overlain and underlain by continental sediments of the Çökek Member. The amount and size of pumice fragments increase from bottom to top.

The Kızılkaya Ignimbrite consists of gray and pinkish-red welded ignimbrite with a well-developed columnar jointing, and it forms the cliffs. There is a basalt fallout

Table 2 The uniaxial compressive strength (UCS) and the four-cycle slake durability index (SDI) test results

Rock code	UCS (MPa)		SDI (%)	
	Average value	Standard deviation	Average value	Standard deviation
1	13.2	3.21	81.3	2.84
2	8.5	1.34	79.7	2.15
3	18.5	2.80	91.9	2.17
4	27.4	2.91	95.9	0.99
5	16.5	2.16	94.2	1.05
6	5.2	0.92	78.2	0.67
7	3.9	0.58	63.6	3.90
8	8.4	2.01	83.0	1.20
9	12.7	0.50	88.4	0.90
10	15.8	2.13	88.3	3.36
11	9.9	1.22	79.7	0.76
12	27.8	2.35	93.4	3.33
13	14.1	2.50	89.0	3.05
14	15.7	2.00	90.8	0.21
15	18.3	1.93	92.7	2.93
16	41.0	2.42	96.3	1.11
17	12.4	1.63	90.2	0.08
18	7.4	0.96	69.4	3.45
19	12.4	1.23	90.3	3.14
20	2.2	0.21	61.2	1.79
21	10.3	1.40	78.0	2. 44
22	9.1	0.51	83.9	2.16
23	8.5	0.82	78.8	0.53
24	7.9	1.10	73.9	4.53
25	8.8	1.10	82.9	3.91
26	36.4	3.70	96.4	1.08
27	25.7	2.61	95.0	2.37
28	18.8	1.10	92.8	2.01
29	23.9	2.01	95.2	1.77
30	44.3	3.23	97.9	0.92
31	46.7	1.30	97.7	3.55

layer with a maximum thickness of 20 cm at the base. It overlies the fluvial-lacustrine deposits of the Çökek Member. Its thickness changes from 5 to 25 m in the study area but locally reaches 70 m.

The mineralogical and structural properties of each sample were determined under the polarizing microscope. These properties are summarized in Table 1.

Experimental studies

Slake durability tests were conducted using ten rounded rock lumps, each with a mass of 40–60 g, as suggested by ISRM (2007). The oven-dried lumps were placed in a standard test drum filled with tap water at about 20 °C and rotated for 200 revolutions during a period of 10 min. The rock pieces retained in the drum were oven dried at 110 °C for 24 h, cooled, and weighed. The samples were subjected to four cycles and the four-cycle slake durability index was calculated. The tests were repeated three times for each rock type and the average value was recorded as the SDI (Table 2).

The UCS tests were carried out on the smooth cut and oven-dried core samples according to ASTM (1986) standards. The tests were repeated at least five times for each rock type and the average value was recorded as the UCS.

Results and discussion

As shown in Table 2, the UCS values range from 2.2 to 46.7 MPa and the SDI values range from 61.2 to 97.9 %. The test results were analyzed using the method of least

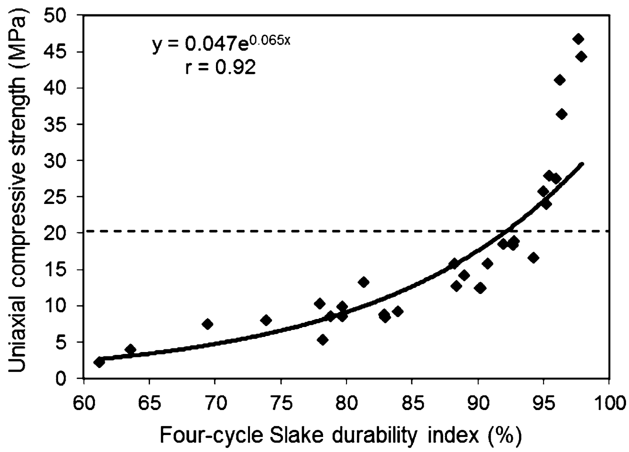

Fig. 2 The correlation between uniaxial compressive strength and four-cycle slake durability index

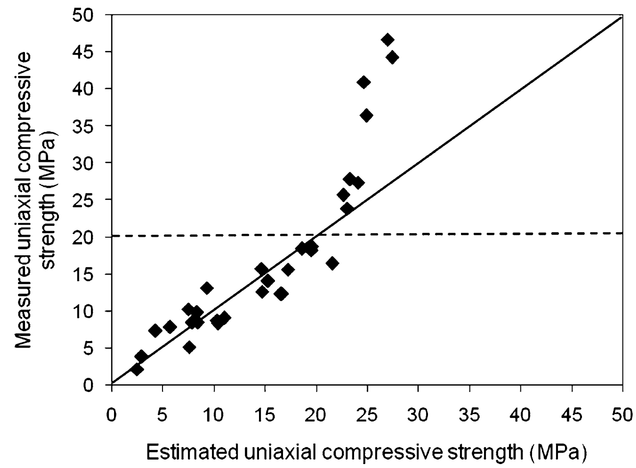

Fig. 3 Measured versus estimated uniaxial compressive strength for Eq. (9)

squares regression. Linear, logarithmic, exponential, and power curve fitting approximations were tried and the best approximation equation with highest correlation coefficient was determined.

A very strong correlation was found between the SDI values and UCS values (Fig. 2). The relations follow exponential function. The equation of the curves is

$$UCS = 0.047e^{0.065I_{d4}} \quad r = 0.92 \tag{9}$$

where UCS is the dry uniaxial compressive strength (MPa), and I_{d4} is the four-cycle SDI (%).

As shown in Fig. 2, the UCS values increase with increasing SDI values. Although, the correlation coefficient of the relation is very strong, the data are scattered over the UCS values of 20 MPa. In order to see the estimation capability of the derived relation, the graph of the estimated UCS versus the predicted UCS was plotted (Fig. 3). The data points are distributed nearly uniformly about the diagonal line below the UCS values of 20 MPa. However, they deviate from the diagonal line and show a different trend over the UCS values of 20 MPa. It is clear that the UCS-SDI correlation indicates different trends above and below the UCS values of 20 MPa for pyroclastic rocks. Therefore, the UCS-SDI correlation plots were redrawn for above and below the UCS values of 20 MPa, respectively. As shown in Fig. 4, there are linear correlations between the SDI values and the UCS values for the two cases. The equations of the lines are

$$UCS = 0.453I_{d4} - 26.22 \quad r = 0.89 \tag{10}$$

$$UCS = 7.75I_{d4} - 711.4 \quad r = 0.93 \tag{11}$$

The correlation coefficients of the equations are very strong. Increasing the SDI values increases the UCS values. However, the slopes of the regression lines are very

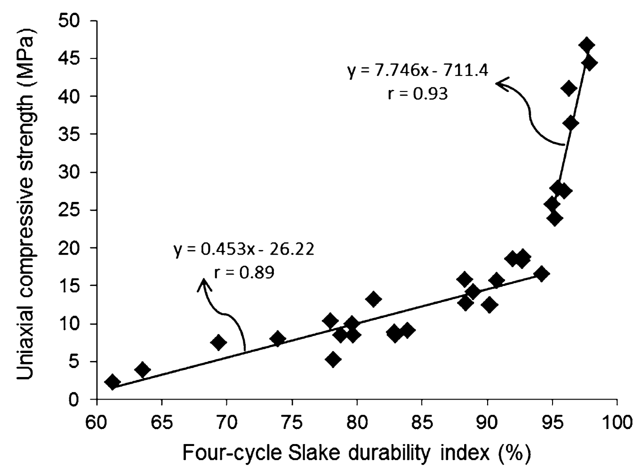

Fig. 4 The correlation between uniaxial compressive strength and four-cycle slake durability index for above and below the UCS values of 20 MPa

different. A slight increase in the SDI values causes too much increase in the UCS values for the second case.

That the correlation coefficients of the derived relations are very good does not necessarily identify the valid model. Therefore, the validation of the derived relations was checked by the *t* test and the *F* test.

The significance of *r* values can be determined by the *t* test, assuming that both variables are normally distributed and the observations are chosen randomly. If the computed *t* value is greater than the tabulated *t* value, the null hypothesis is rejected. This means that *r* is significant. If the computed *t* value is less than tabulated *t* value, the null hypothesis is not rejected and *r* is not significant. As seen in Table 3, the computed *t* values are greater than the tabulated *t* values, suggesting that the models are valid.

Table 3 *t* and *F* test results

Eq. no	*t* table	*t* test	*F* table	*F* test
10	±2.07	62.87	4.06	1105.28
11	±2.36	21.77	4.60	370.24

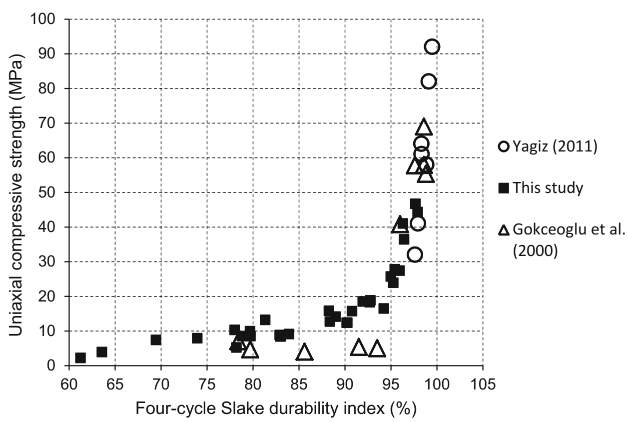

Fig. 5 The comparison of the data of this study to the data of Yagiz (2011) and Gokceoglu et al. (2000)

To test the significance of the regressions, analysis of variance (ANOVA) for the regression was employed. If the computed *F* value is greater than tabulated *F* value, the null hypothesis is rejected that there is a real relation between dependent and independent variables. As shown in Table 3, the computed *F* values are greater than the tabulated *F* values. It is concluded from those statistical considerations that the models are significant according to the *F* test.

Because Yagiz (2011) and Gokceoglu et al. (2000) performed four-cycle SDI tests, their data are suitable to compare with the data of this study. Figure 5 shows the data points of the three studies in one plot. The data points of Yagiz (2011) and Gokceoglu et al. (2000) conform generally well to the data points of this study. Three or two data points from Gokceoglu et al. (2000) indicate scattering. These data points also show scattering in the correlation plot drawn by Gokceoglu et al (2000). They stated that "The scattered data correspond to laminated marl samples that easily disintegrate due to the presence of laminae and yield high SDI values even though their strength is considerably low."

Conclusions

The possibility of predicting UCS from SDI was investigated for pyroclastic rocks. The UCS values were correlated with the SDI values and a very strong exponential relation was found between the two parameters. However, it was seen that some data were scattered over the UCS values of 20 MPa. For this reason, the correlation graph between the UCS and SDI values was replotted for above and below the UCS values of 20 MPa, respectively. The linear relations for two cases have very strong correlation coefficients and the data points are not scattered. The derived equations are also significant according to the statistical tests.

It was concluded that the UCS of pyroclastic rocks can be estimated from the SDI. Because the data were collected from the large CPV having a long axis of about 300 km and because the area has very different volcanic materials, the derived relations can be generalized.

Acknowledgments This work was supported by the Turkish Academy of Sciences within the framework of the Young Scientist Award Program. (EA-TUBA-GEBIP/2001-1-1).

References

ASTM (1986) Standard test method of unconfined compressive strength of intact rock core specimens. D2938

Bonelli R (1989) Relationship between engineering properties and petrographic characteristics of selected sandstones. MSc. Thesis, Ohio: Kent State University

Cargill JS, Shakoor A (1990) Evaluation of empirical methods for measuring the uniaxial compressive strength of rock. Int J Rock Mech Min Sci 27:495–503

Dincer I, Acar A, Ural S (2008) Estimation of strength and deformation properties of quaternary caliche deposits. Bull Eng Geol Environ 67:353–366

Gokceoglu C, Ulusay R, Sonmez H (2000) Factors affecting the durability of selected weak and claybearing rocks from Turkey, with particular emphasis on the influence of the number of drying and wetting cycles. Eng Geol 57:215–237

ISRM (2007) The complete ISRM suggested methods for rock characterization, testing and monitoring: 1974–2006. Suggested methods prepared by the commission on testing methods. In: International Society for Rock Mechanics, Ulusay R and Hudson JA (eds) Compilation arranged by the ISRM Turkish National Group, Ankara, Turkey, Kozan Ofset

Koncagul EC, Santi PM (1999) Predicting the unconfined compressive strength of the Breathitt shale using slake durability, shore hardness and rock structural properties. Int J Rock Mech Min Sci 36:39–153

Sayin MN (2008) Fairy chimney development in Cappadocian ignimbrites (Central Anatolia, Turkey). Ph.D. Thesis, Middle East Technical University. p 137

Toprak V, Keller J, Schumacher R (1994) Volcano-tectonic features of the Cappadocian volcanic province. International Volcanological Congress—excursion guide, Ankara (Turkey). Middle East Technical University, Ankara

Yagiz S (2011) Correlation between slake durability and rock properties for some carbonate rocks. Bull Eng Geol Environ 70:377–383